 Bull. Chem. Soc. Jpn. Vol. 81, No. 12, 1669–1674 (2008)

Improvement of Co_3O_4 Nanoparticle Synthesis in Apoferritin Cavity by Outer Surface PEGylation

Rikako Tsukamoto,[1,2] Masahiro Muraoka,[1,3] Yoshitsugi Fukushige,[1,2] Hiromichi Nakagawa,[1,2] Tomohiro Kawaguchi,[3] Yohji Nakatsuji,[3] and Ichiro Yamashita*[1,2,3]

[1]CREST, Japan Science and Technology Agency, Honcho, Kawaguchi 332-0012

[2]Graduate School of Materials Science, Nara Institute of Science and Technology, Takayama, Ikoma 630-0192

[3]Department of Applied Chemistry, Faculty of Engineering, Osaka Institute of Technology, Omiya, Asahi-ku, Osaka 535-8585

Received June 12, 2008; E-mail: ichiro@ms.naist.jp

The outer surface of horse spleen apoferritin (HsAFr) was chemically modified by poly(ethylene glycol) (PEG) to prevent bulk precipitation during artificial biomineralization of the cobalt-oxide core (Co_3O_4) in its cavity. Two kinds of PEGs, with average molecular weights of 2000 and 5000 were covalently attached (PEGylation) on the outer surface of HsAFr and suppressed the bulk precipitation drastically, whereas neither free PEGs nor short PEG (*N*-{2-[2-(2-methoxy-ethoxy)ethoxy]ethanoyloxy}succinimide) performed such suppression. The PEGylated HsAFr accommodated fully developed Co_3O_4 cores and achieved a high yield of homogeneous Co_3O_4 nanoparticles. Investigation of the early biomineralization stage suggested that [$Co^{III}O$] complex ions were accumulated around the negatively charged outer surface of HsAFr.

Nanoparticles (NPs) have unprecedented, sophisticated, and useful properties that cannot be attained by bulk materials due to the significantly high ratio of their surface to volume and/or ultra small size. Conductive and semiconductive NPs, particularly are attracting research interest from the viewpoint of nanoelectronic devices. The electron energy levels of conductive and semiconductive NPs are quantized according to their sizes and they play an essential role as quantum dots in nanoelectronic devices. Since the electron energy levels are very sensitive to NP size, the homogeneity of NPs is crucial but hard to achieve. To address this issue, a cage-shaped protein, apoferritin has been employed and its cavity was utilized as a spatially restricted chemical-reaction chamber for NP synthesis. The NPs synthesized and fully developed in the cavity had the same size and shape. Many kinds of inorganic NPs have been produced in the apoferritin cavity in vitro[1–12] and some NPs were successfully used in nanoelectronic devices.[13–16] Moreover, the protein shell has been used as a vehicle to deliver the NP to a designated place or to make ordered structures for future applications.[17–19]

Apoferritin is a major cellular iron-storage protein that consists of 24 polypeptide subunits. Figure 1 is a schematic drawing of the protein looking along the four-fold axis and its cross section. The inner and outer diameters of the protein shell are about 7 and 12 nm, respectively. Hydrophilic channels along the three-fold axis connect the cavity to the outside. The channel has a diameter of 0.3–0.4 nm and is responsible for transporting iron ions. The inner cavity can store up to about 4000 iron atoms in a ferrihydrite core in vivo.[20,21] Previous studies have indicated that the electrostatic potential profile produced mainly by the negatively charged amino acids on the inner surface enhances the introduction of the positive iron ions into the cavity.[22] Meldrum et al. reported that the outer surface of horse spleen apoferritin (HsAFr) suppressed bulk precipitation but the inner surface enhanced mineralization, phenomenon known as the "Janus effect."[3] Iwahori et al. also described the mechanism of semiconductor (CdSe,CdS) NP synthesis in the apoferritin cavity.[8]

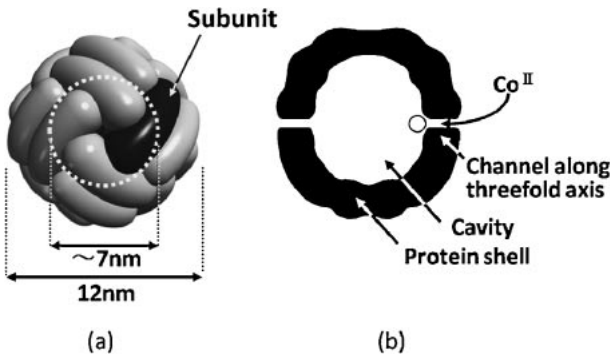

Figure 1. Schematic drawing of apoferritin molecule: (a) viewed down a four-fold axis and (b) cross section including two three-fold channels.

Among a variety of NPs synthesized in the apoferritin cavity, Co_3O_4 nanoparticles were of interest as possible components of nano-electronics. It is a wide-gap semiconductor and has been used for charge-storage nodes for a floating gate memory.[13] Douglas et al. reported the biomineralization of cobalt nanoparticles in the HsAFr. Cobalt hydroxide oxide, CoO(OH) and Co_3O_4 core was formed in the HsAFr by oxidizing Co^{II} with H_2O_2. The reaction solution was dynamically ti-

Published on the web December 12, 2008; doi:10.1246/bcsj.81.1669

trated at pH 8.5 using NaOH. They also fabricated smaller cobalt nanoparticles in an apoferritin-like protein, Dps from Listeria innocua via the same method.[23,24] However, dynamic titration can not make large quantities of cobalt oxide nanoparticles. In our previous work, we reported the one-pot synthesis of Co_3O_4 cores with a narrow size distribution in the horse spleen apoferritin cavity using buffer solution (Co-feritin), which is suitable for mass-production.[9]

Co-ferritins were made into a two-dimensional array on a MOSFET channel. After selective protein elimination and embedding in a SiO_2 layer, the array of NPs successfully functioned as memory nodes of a floating-nanodots gate memory.[13]

However, the one-pot synthesis of Co_3O_4 NPs in the apoferritin cavities was accompanied by a significant amount of bulk precipitation, resulting in coprecipitation of Co-ferritin.[9] A method for preventing the bulk precipitation is needed to achieve a high yield of Co-ferritin and it was anticipated that some modification of the outer surface of apoferritin would be necessary. Mann et al. reported that the modification of alkylate groups on the outer surface of ferritin allowed it to disperse in organic solvent.[25] In this work, we covalently attached poly(ethylene glycol) (PEG) on the outer surface of apoferritin (PEGylation) to alter its characteristics of the outer surface.[30] PEGylation is widely used to make surfaces biocompatible and prevent protein aggregations.[26–29] We report here that the PEGylation of apoferritin suppressed bulk precipitation drastically and improved the yield of Co-ferritin significantly. There was no discernable effect of PEGylation on Co_3O_4 core formation. Based on the experimental results, the mechanism of Co_3O_4 biomineralization could be proposed.

Experimental

PEGylation of Apoferritin Molecules. Horse spleen apoferritin (HsAFr) was purchased from SIGMA-Aldrich and purified by gel filtration. The HsAFr was modified by using two kinds of PEG derivatives, the mean molecular weights (MW) of which are 2 and 5 kDa, respectively. The general procedure for the chemical modification of ferritin with PEG derivatives is described elsewhere.[30] In short, HsAFr was reacted with MeO–PEG–NHS to generate an amide ester of the PEG derivatives exposed on the exterior surface. This reaction covalently attached PEG molecules to the lysine residues on the outer surface of ferritin. Six milligrams of HsAFr (13 nmol) was incubated overnight with about 800 mol excess of the PEG derivatives per apoferritin subunit at 4 °C in 30 mL of 100 mM (1 M = 1 mol dm^{-3}) phosphate buffer pH 8.2. The buffer was exchanged to 150 mM NaCl and concentrated using ultrafiltration membranes. The exchange process was repeated more than twenty times. The purity of the products was confirmed by analytical size-exclusion chromatography (SEC) using a gel-filtration column (G4000 SWXLPEEK, TOSOH). The stoichiometry (PEG/subunit) of the apoferritin derivative was determined by time-of-flight mass spectrometry (MALDI-TOFMS, Voyager-DETM STR, Applied Biosystems).

Biomineralization of Co_3O_4 Ferritin Core. The general procedure for the optimal Co_3O_4 core formation is described elsewhere.[9] The apoferritin proteins were dissolved in 100 mM of HEPES pH 8.3, with 37.5 mM of Na_2SO_4 to a final concentration of 0.5 mg mL^{-1} (1 μM). In this study, ammonium cobalt sulfate (ACS) was added to a final concentration of 2 to 9 mM, followed by the addition of H_2O_2 with a half-stoichiometric concentration of ACS to oxidize Co^{II}. The solution was stirred and incubated for about 20 min at room temperature and then overnight at 50 °C in a temperature-controlled aluminum box. The solution after synthesis of Co_3O_4 NP was centrifuged at low speed to remove precipitates. The protein concentration of the supernatant was determined using a Bradford protein assay kit (Bio-Rad). The core formation was confirmed by transmission electron microscopy (TEM) with negative staining using 1% aurothioglucose which does not stain the inside of the cavity. Since aurothioglucose has a fairly fast background nanogold formation when irradiated by an electron beam, we also carried out TEM observation using samples stained with phosphotungstic acid (PTA). The core formation ratio (CFR) was calculated by dividing the number of core-containing apoferritins by the number of all apoferritins in the TEM images and was used for evaluating core-formation efficiency. The yield of the ferritin ratio (YFR) was the ratio of the final protein concentration of core formed ferritin in the supernatant to the initial apoferritin concentration, i.e. YFR = (The protein concentration in the supernatant after core formation × CFR) ÷ the initial apoferritin concentration.

Ultrafiltration and Resonance Raman Spectra. The reaction solution left for 20 min at room temperature after mixing was washed with distilled water. Concentration using ultrafiltration membranes with a cut-off molecular weight of 50 kDa (Centriprep YM50/Millipore) and dilution with pure water was repeated several times. The color of the solution containing molecules greater than 50 kDa was brown and the solution with less than 50 kDa was colorless and transparent. Resonance Raman spectra were obtained from the solution that did not pass through the 50 kDa cut off membrane using a NSR-2100 (JASCO). The 514.5 nm line of an Ar^+ laser was used as the exciting source. The laser power was 10 mW.

Results and Discussion

PEGylation of HsAFr. The PEGylation of HsAFr was examined by size-exclusion chromatography. Figure 2 shows the elution profile of the HsAFr and PEGylated HsAFr. The void volume was 6.6 mL. The elution volume of HsAFr (about 450 kDa) was 10.3 mL. The PEGylated apoferritin was eluted with a volume of 10.0 mL for the HsAFr-2000 and 9.0 mL for the HsAFr-5000. These results indicated that the PEGylated HsAFrs became larger and HsAFr-5000 was bigger than HsAFr-2000, as expected. The number of the PEG molecules

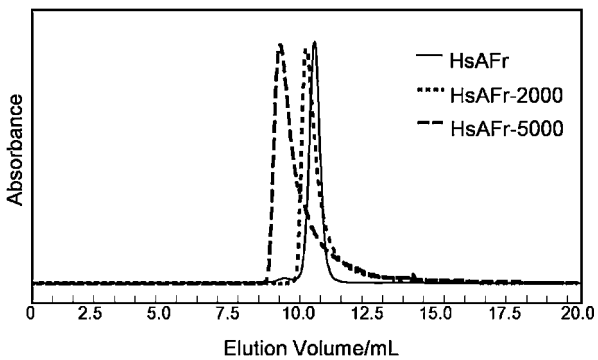

Figure 2. Size-exclusion chromatography of native and PEGylated apoferritins. Vertical axis is absorbance at 280 nm (arbitrary units). The PEGylated apoferritin was eluted with a smaller volume according to the average size of the attached PEG.

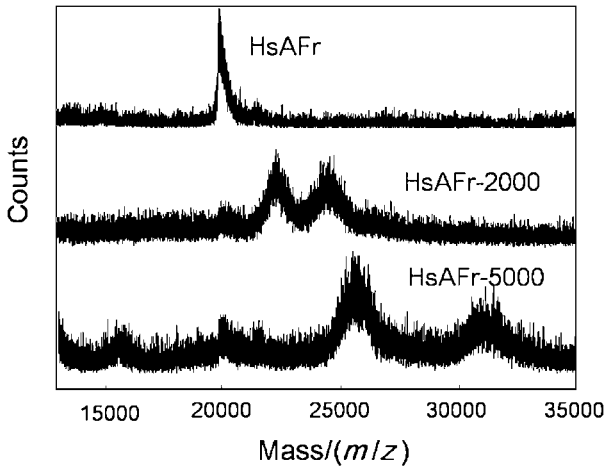

Figure 3. MALDI-TOFMS spectra of native and PEGylated apoferritins. The native apoferritin shows a single peak at around 20 kDa while the PEGylated apoferritins have two additional peaks. The weight increases correspond to one or two PEG molecules covalently attached to the HsAFr.

attached to the HsAFr was estimated by MALDI-TOFMS. The peak of the HsAFr, HsAFr-2000, and HsAFr-5000 are shown in Figure 3. The HsAFr's subunits and PEGylated HsAFr's subunits can be easily distinguished by the weight changes. The HsAFr shows a sharp single peak around 20 kDa that corresponds to the molecular weight of the native apoferritin subunit. HsAFr-2000 and HsAFr-5000 show one small peak which corresponds to unmodified subunits and two large peaks. In the case of HsAFr-2000, the weight increase interval was about a 2 kDa, and HsAFr-5000 showed an increase of approximately 5 kDa. From these results we assume that the lighter molecule is the subunit with one PEG molecule, and the heavier molecule is the subunit with two PEG molecules. Almost all the PEGylated HsAFr subunits have one or two covalently attached PEG molecules, i.e. each HsAFr has 24 to 48 PEG molecules. There are no peaks corresponding to subunits with more than two PEG molecules, although each subunit has more than two reactive amino acids (Lys) on the outer surface. This suggested that steric hindrance limits the number of attached PEG molecules and that the apoferritin surface is entirely coated by PEG.

Precipitation Suppression by PEGylation during Co_3O_4 Biomineralization. Using 1 μM of HsAFr, HsAFr-2000, and HsAFr-5000, biomineralization of Co_3O_4 was carried out in a reaction solution of 100 mM of HEPES pH 8.3, 37.5 mM of Na_2SO_4, and ammonium cobalt sulfate (ACS) with concentrations from 2 to 9 mM with hydrogen peroxide (H_2O_2) at half the concentration of ACS.

Figure 4a shows the reaction solutions with 5 mM of ACS after 20 min incubation at room temperature. From left to right in Figure 4, the solutions contained HsAFr, HsAFr-2000, HsAFr-5000, and no protein. Upon the addition of H_2O_2, the color of the solutions changed from a light pink to a light brown, accompanying the oxidation of the divalent cobalt ions. The states of the solutions after 20 min were the same, except the solution without proteins which became turbid due to cobalt oxide precipitation. It was clearly seen that HsAFr and

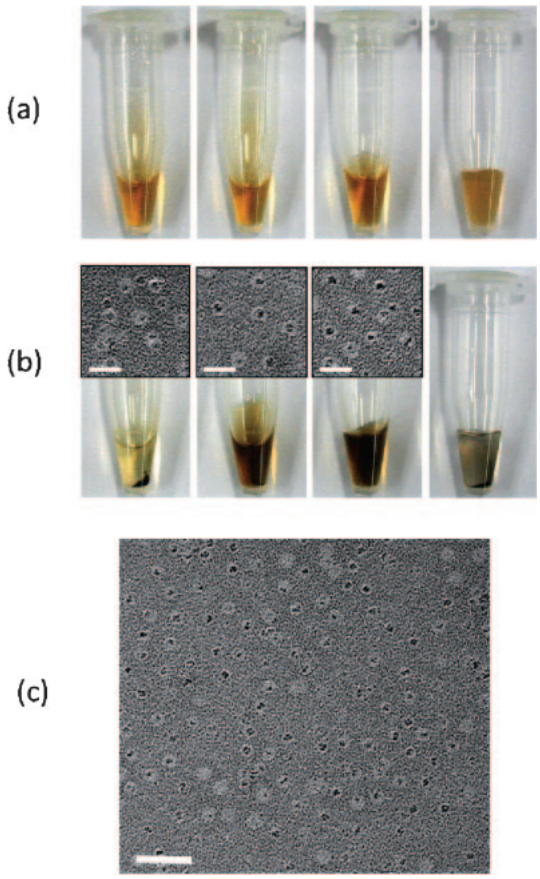

Figure 4. State of a reaction solution with 5 mM of ACS, (a) 20 min after the addition of H_2O_2 and (b) after a 16-h incubation at 50 °C. In each figure, from left to right, solutions contain the native HsAFr, HsAFr-2000, HsAFr-5000, and no protein. Insets are TEM images of the Co_3O_4 core formed with native HsAFr, HsAFr-2000, and HsAFr-5000 stained by aurothioglucose. The scale bar is 30 nm. (c) TEM image of the HsAFr-5000 after Co_3O_4 core synthesis. Stained by aurothioglucose. The scale bar is 50 nm.

the PEGylated HsAFr repressed the bulk precipitation and the solutions remained clear.

Figure 4b shows the reaction solutions after 16-h incubation at 50 °C. The solutions were centrifuged at low speed and the precipitates were made into pellets. The reaction solution without proteins showed heavy precipitation and made a hard pellet. Some precipitates adhered to the tube wall. The retrieved supernatant was totally transparent, indicating that all cobalt ions became an insoluble cobalt oxide precipitate. The solution with HsAFr showed a small amount of precipitation and made a soft, large volume pellet, suggesting that the proteins had co-precipitated. The supernatant was light brown and TEM observation showed that it contained Co-ferritins. Figure 4c shows a larger frame TEM image of the Co_3O_4 core formed with HsAFr-5000. The HsAFr has been reported to have the ability to suppress bulk precipitation during the selective manganese-core formation in the cavity.[3] This result showed that HsAFr has a similar repression effect against Co_3O_4 bulk precipitation. Contrary to the previous two cases, no precipitation occurred in the solution containing PEGylated HsAFrs. The color changed from light to dark brown, but the supernatant re-

mained clear, indicating that the cobalt ion or cobalt nanoparticles had been dispersed in the solution. It was clear that the PEGylation had an enhanced suppression effect on the bulk precipitation.

The insets in Figure 4b are TEM images of HsAFr-2000 and HsAFr-5000 stained with aurothioglucose after a 16-h incubation at 50 °C. Both images show Co_3O_4 cores surrounded by a protein shell carrying PEG molecules, which were negatively stained as a white ring. The TEM images clearly showed that PEGylation did not affect the core formation. PEGylated HsAFrs efficiently formed Co_3O_4 cores.

Improvement of Co-Ferritin Yield by PEGylation. To evaluate the improvement of Co_3O_4 core formation efficiency, we studied the ratio of the final protein concentration of core formed ferritin in the supernatant to the initial apoferritin concentration, which we named yield of ferritin ratio (YFR). Varying the ACS concentration, the protein concentration of the supernatant was measured by the Bradford method and core formation ratio (CFR) was determined by analysis of TEM images. Using these results, YFR was calculated as the product of CFR and protein concentration of the supernatant.

Figure 5 shows the dependence of protein concentration and YFR on ACS concentration. In the case of HsAFr, the final protein concentration in the supernatant was much lower than PEGylated HsAFr (Figure 5a). Reflecting this result, a YFR of about 40% at 2 mM ACS sharply decreased as ACS concentration increased and became negligible around 6 mM (Figure 5b). In the case of HsAFr-2000, the final protein concentration in the supernatant was significantly higher than that in HsAFr, and also slowly decreased as ACS concentration increased. This result is consistent with the fact that the formation of the bulk precipitate was suppressed by PEGylation. Due to the drastic increase in the supernatant protein concentration (Figure 5a), YFR was significantly improved, that is, a YFR of about 50% was achieved at ACS concentrations between 3 and 5 mM (Figure 5b). Similar results were obtained with HsAFr-5000 and it showed a wider ACS concentration range in which YFR remained higher compared to HsAFr-2000.

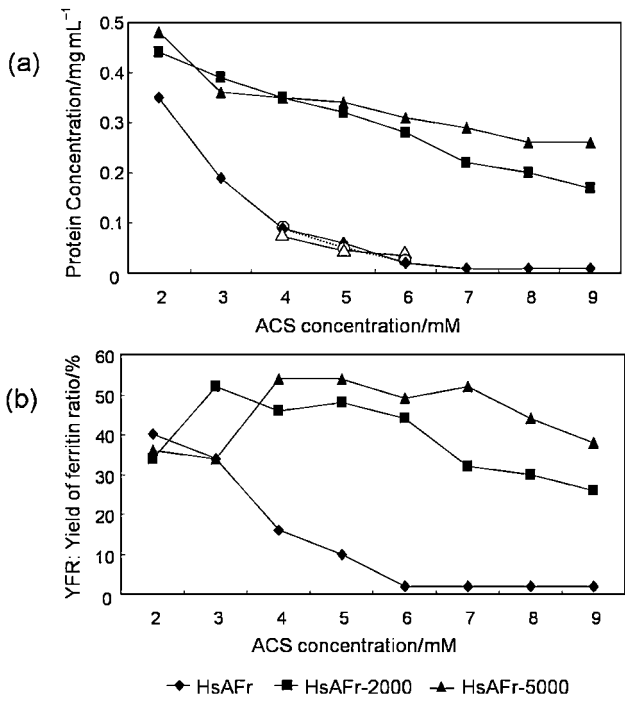

Figure 5. Dependence of protein concentration in the supernatant and YFR after 16-h incubation at 50 °C. (a) Protein concentration, (b) YFR.

Evidence of Bulk Precipitation Suppression by PEGylation. To clarify whether PEG molecule itself, or free PEG molecules have the ability to suppress bulk precipitation, we conducted Co_3O_4 biomineralization with 1 μM of HsAFr and 100 μM of PEG-2000 instead of 1 μM of PEGylated apoferritins. This corresponds to 100 PEG molecules per apoferritin molecule, which is slightly more PEGs than in PEGylated apoferritin. ACS concentration was between 4 and 6 mM. The open circles in Figure 5a show the supernatant-protein concentrations, which were the same as those in the HsAFr. The result indicated that the presence of free PEG-2000 did not have the ability to repress bulk precipitation. PEG molecules need to be covalently attached to the apoferritin surface.

Since our PEGylation method used lysine residues, there was a possibility that the loss of positively charged lysines changed the electrostatic potential and suppressed the bulk precipitation. Hence, we modified the apoferritins using short PEG (*N*-{2-[2-(2-methoxyethoxy)ethoxy]ethanoyloxy}succinimide). The modification was confirmed by MALDI-TOFMS (data not shown). Co_3O_4 biomineralization experiments were carried out using the same conditions described above and an ACS concentration of between 4 and 6 mM. The supernatant-protein concentrations were the same as those in the HsAFr (the open triangles in Figure 5a). The result shows that the loss of the lysine charge did not affect the bulk precipitation.

The data above clearly confirmed that PEG has to be covalently attached to the outer surface of the apoferritin shell to enhance the suppression of bulk precipitation.

Elucidation of the Mechanism of Bulk Precipitation Suppression. To elucidate the mechanism of the bulk precipitation suppression, we first investigated the early stage of the Co_3O_4 biomineralizaion, i.e. room-temperature incubation. The reaction solutions of HsAFr or PEGylated HsAFr changed their color from light pink to clear brown after addition of H_2O_2 accompanying the oxidation of Co^{II} ions. After 20-min incubation the solution became stable and precipitate was not seen even after overnight incubation. TEM observation of the solution after 20-min incubation at room temperature showed only apoferritin. No difference was seen between HsAFr and PEGylated HsAFr.

The reaction solution with HsAFr after 20-min incubation was ultrafiltered using a membrane with a cut-off molecular weight of 50 kDa. The solution containing HsAFr was clear brown but without HsAFr was totally transparent. Therefore, it was suggested that the solution with HsAFr contained some forms of Co oxide complex ions and that Co oxide complex ions and HsAFr interacted with each other to form stable conjugates.

We carried out resonance Raman spectra measurement of the conjugate (HsAFr with Co oxide complex ions) in distilled water. The peak observed at 500–650 cm^{-1} was assigned to the

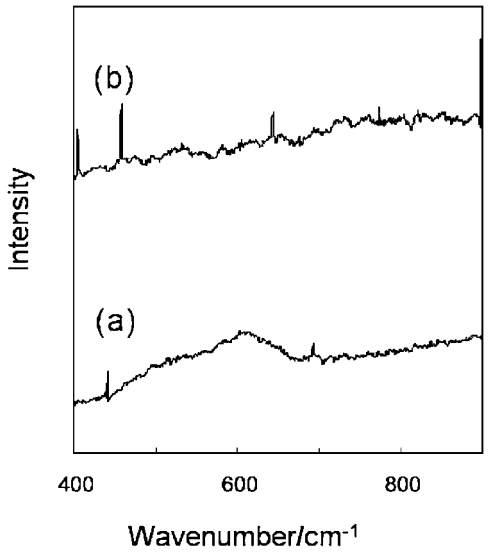

Figure 6. (a) Resonance Raman spectra of a solution washed with distilled water after being incubated for 20 min at room temperature. (b) HsAFr alone in distilled water.

Co–O stretching vibrations (Figure 6a),[31] which were not observed from HsAFr alone in distilled water. (Figure 6b). This peak indicated the existence of [$Co^{III}O$] complex ions.

When the incubation temperature was elevated to 50 °C, in the case of HsAFr, core formation and bulk precipitation started simultaneously but in the case of PEGylated HsAFr, core formation started without bulk precipitation. We suggested that [$Co^{III}O$] complex ions decomposed into Co^{III} ions upon temperature elevation and the produced Co^{III} ions entered the cavity to form Co_3O_4 cores. It may also be the case that the attached PEG molecules stabilize decomposed Co^{III} ions and prevented bulk precipitation. But where PEG is absent, decomposed Co^{III} ions were not stabilized enough and bulk precipitation began.

Based on these results, we propose the mechanism of core formation as follows. Stable positively charged [$Co^{III}O$] complex ions are produced by the addition of H_2O_2. The produced [$Co^{III}O$] complex ions are accumulated around the negatively charged outer surface (Zeta potential; −21 mV, pH 7) of HsAFr or PEGylated HsAFr by electrostatic interaction.[32] PEG chains might accommodate more [$Co^{III}O$] complex ions. When temperature is elevated to 50 °C, [$Co^{III}O$] complex ions decompose into reactive Co^{III} ions but the spaces among PEG chains accommodate these ions stably, consequently suppressing bulk precipitation. [$Co^{III}O$] ions released in the vicinity of apoferritin go through the three-fold channel into the apoferritin cavity, where Co_3O_4 nuclei are produced at the nucleation sites.

Conclusion

The PEGylation of HsAFr was performed using the chemical reaction of MeO–PEG–NHS with Lys amino-acid residues on the outer surface of the HsAFr protein shell. Modification of the outer surface by PEG molecules with molecular weights of 2000 and 5000 Da dramatically suppressed bulk precipitation. PEGylated HsAFr can biomineralize the Co_3O_4 core in the same way as native HsAFr. Due to the suppression of the bulk precipitation, the PEGylated HsAFr achieved a high yield of Co_3O_4 homogeneous nanoparticles, and HsAFr-5000 is more effective than HsAFr-2000. We propose that Co_3O_4 core formation in the cavity of HsAFr has two phases. At first, the produced [$Co^{III}O$] complex ions are attracted by the negatively charged HsAFr outer surface and accommodated in the spaces among PEGs. Secondly, the [$Co^{III}O$] complexes ions become unstable at 50 °C and the generated Co^{III} ions pass through the three-fold channel and mineralize. The results obtained in this study will supply important additional information about the Janus effect of apoferritin biominealization and will allow further improvement of YFR.

References

1 S. Mann, F. C. Meldrum, *Adv. Mater.* **1991**, *3*, 316.
2 F. C. Meldrum, V. J. Wade, D. L. Nimmo, B. R. Heywood, S. Mann, *Nature* **1991**, *349*, 684.
3 F. C. Meldrum, T. Douglas, S. Levi, P. Arosio, S. Mann, *J. Inorg. Biochem.* **1995**, *58*, 59.
4 T. Douglas, D. P. E. Dickson, S. Betteridge, J. Charnock, C. D. Garner, S. Mann, *Science* **1995**, *269*, 54.
5 T. Douglas, V. T. Stark, *Inorg. Chem.* **2000**, *39*, 1828.
6 M. Okuda, K. Iwahori, I. Yamashita, H. Yoshimura, *Biotechnol. Bioeng.* **2003**, *84*, 187.
7 I. Yamashita, J. Hayashi, M. Hara, *Chem. Lett.* **2004**, *33*, 1158.
8 K. Iwahori, K. Yoshizawa, M. Muraoka, I. Yamashita, *Inorg. Chem.* **2005**, *44*, 6393.
9 R. Tsukamoto, K. Iwahori, M. Muraoka, I. Yamashita, *Bull. Chem. Soc. Jpn.* **2005**, *78*, 2075.
10 K. Yoshizawa, K. Iwahori, K. Sugimoto, I. Yamashita, *Chem. Lett.* **2006**, *35*, 1192.
11 J.-W. Kim, S. H. Choi, P. T. Lillehei, S.-H. Chu, G. C. King, G. D. Watt, *Chem. Commun.* **2005**, 4101.
12 H.-A. Hosein, D. R. Strongin, M. Allen, T. Douglas, *Langmuir* **2004**, *20*, 10283.
13 H. Kirimura, Y. Uraoka, T. Fuyuki, M. Okuda, I. Yamashita, *Appl. Phys. Lett.* **2005**, *86*, 262106.
14 A. Miura, T. Hikono, T. Matsumura, H. Yano, T. Hatayama, Y. Uraoka, T. Fuyuki, S. Yoshii, I. Yamashita, *Jpn. J. Appl. Phys.* **2006**, *45*, L1.
15 K. Ichikawa, Y. Uraoka, P. Punchaipetch, H. Yano, T. Hatayama, T. Fuyuki, I. Yamashita, *Jpn. J. Appl. Phys.* **2007**, *46*, L804.
16 T. Kubota, T. Hashimoto, M. Takeguchi, K. Nishioka, Y. Uraoka, T. Fuyuki, I. Yamashita, S. Samukawa, *J. Appl. Phys.* **2007**, *101*, 124301.
17 I. Yamashita, H. Kirimura, M. Okuda, K. Nishio, K. Sano, K. Shiba, T. Hayashi, M. Hara, Y. Mishima, *Small* **2006**, *2*, 1148.
18 S. Kumagai, S. Yoshii, K. Yamada, N. Matsukawa, I. Fujiwara, K. Iwahori, I. Yamashita, *Appl. Phys. Lett.* **2006**, *88*, 153103.
19 T. Matsui, N. Matsukawa, K. Iwahori, K. Sano, K. Shiba, I. Yamashita, *Langmuir* **2007**, *23*, 1615.
20 W. H. Massover, *Micron* **1993**, *24*, 389.
21 D. M. Lawson, P. J. Artymiuk, S. J. Yewdall, J. M. A. Smith, J. C. Livingstone, A. Treffry, A. Luzzago, S. Levi, P. Arosio, G. Cesareni, C. D. Thomas, W. V. Shaw, P. M. Harrison, *Nature* **1991**, *349*, 541.
22 T. Takahashi, S. Kuyucak, *Biophys. J.* **2003**, *84*, 2256.
23 T. Douglas, T. K. Stark, *Inorg. Chem.* **2000**, *39*, 1828.

24 M. Allen, D. Willits, M. Young, T. Douglas, *Inorg. Chem.* **2003**, *42*, 6300.
25 K. K. W. Wong, H. Cölfen, N. T. Whilton, T. Douglas, S. Mann, *J. Inorg. Biochem.* **1999**, *76*, 187.
26 S. Zalipsky, *Adv. Drug Delivery Rev.* **1995**, *16*, 157.
27 A. Abuchowski, T. Van Es, N. C. Palczuk, F. F. Davis, *J. Biol. Chem.* **1977**, *252*, 3578.
28 Q. Wang, K. S. Raja, K. D. Janda, T. Lin, M. G. Finn, *Bioconjugate Chem.* **2003**, *14*, 38.
29 K. S. Raja, Q. Wang, M. J. Gonzalez, M. Manchester, J. E. Johnson, M. G. Finn, *Biomacromolecules* **2003**, *4*, 472.
30 Y. Fukushige, M. Muraoka, I. Yamashita, *Mater. Res. Soc. Jpn.* **2005**, *30*, 549.
31 S. Hikichi, H. Komatsuzaki, N. Kitajima, M. Akita, M. Mukai, T. Kitagawa, Y. Moro-oka, *Inorg. Chem.* **1997**, *36*, 266.
32 T. Douglas, D. R. Pipoll, *Protein Sci.* **1998**, *7*, 1083.